Mon. Not. R. astr. Soc. (1985) **214,** 97–107

Frequency drift in pulsar scintillation

F. G. Smith and N. C. Wright *University of Manchester, Nuffield Radio Astronomy Laboratories, Jodrell Bank, Macclesfield, Cheshire SK11 9DL*

Accepted 1984 December 17. Received 1984 December 4; in original form 1984 May 24

Summary. The dynamic spectra of interstellar scintillation at 408 MHz in 32 pulsars give values for bandwidth and time-scale, and for the characteristic rate of frequency drifting in spectral features. Frequency drift in scintillation patterns is related to large-scale structure in the electron density variations in the medium, while the bandwidth and time-scale of scintillation depend on smaller scale structure. A comparison of these two types of pattern characteristics show conformity with a Kolmogorov spectrum of irregularities extending over a range of scales from 10^9 to 10^{12} m.

1 Introduction

Scintillation of the radio frequency signals from pulsars is usually observed as random fading over periods of some minutes. The fading pattern varies with radio frequency, and the structure of the radio frequency spectrum often shows an organised and consistent drift in frequency (Ewing *et al.* 1970; Manchester & Taylor 1977; Armstrong & Rickett 1981). Scintillation itself is attributable to components of irregularities in the interstellar medium (ISM) with typical sizes of order 10^9 m; the frequency drift is, however, associated with a larger scale, possibly of order 10^{12} m. A further manifestation of irregular diffraction is a slow fluctuation in signal strength, over typical periods of some weeks, which has been attributed to large-scale irregularities, again with scale of order 10^{12} m (Rickett, Coles & Bourgois 1984). It has been suggested that the ISM has a continuous spectrum of electron density fluctuations that closely resembles a Kolmogorov power-law (Lee & Jokipii 1975), and that spectral drifting then results from a range of scale sizes which are too large to cause multipath scattering (Shishov 1973).

Although systematic frequency drifting is observed in many pulsars, the relation to scintillation has not yet been clearly demonstrated. We show in this paper that the rate of frequency drifting can be related to such parameters as pulsar distance and velocity in the same way as the characteristics of scintillation. We are therefore able to compare measured characteristics in scintillation and frequency drifting, and thereby relate the characteristics of the interstellar medium at large and small scales. We show that the spatial spectrum of the electron density irregularities is close to that expected from a Kolmogorov power-law.

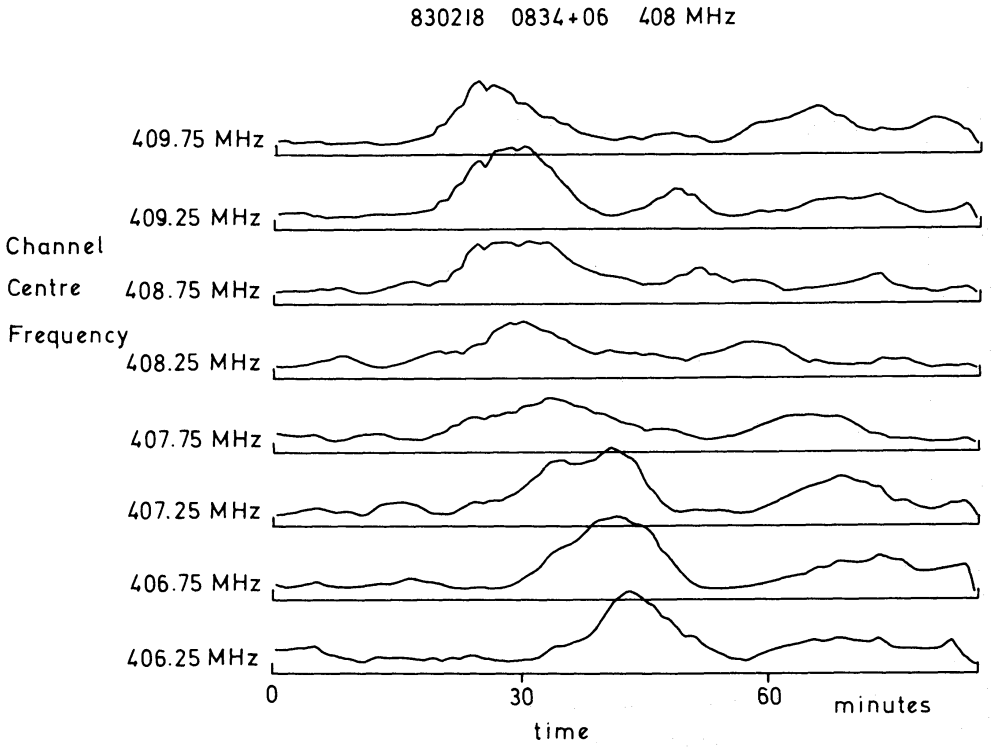

Figure 1. Main pulse intensity for PSR 0834+06 recorded in eight adjacent frequency channels centred on 408 MHz. The observations span 86 min.

2 Observations

Observations were made using the MK IA telescope at 408 MHz and, for some pulsars, at 960 MHz. The receiver bandwidth was divided by analogue filters to eight adjacent bands, either 125 or 500 kHz wide, delayed and dedispersed according to the known dispersion measure of each pulsar. A full pulse profile was recorded for each band, integrated typically through a period of 1 min. In subsequent analysis the pulse power was found by integrating over the main pulse profile, and the fading curve for each frequency band was obtained for observing periods of typically 3 hr.

The data from the eight bands, sampled at intervals of 1 min, formed a two-dimensional array which we refer to as the dynamic spectrum. Fig. 1 shows a typical dynamic spectrum. A two-dimensional autocorrelation function of this array was formed, giving a measure of the scintillation bandwidth and time-scale, and also displaying any measurable frequency drifts. These parameters were derived by fitting Gaussian curves to the autocorrelation functions. The scintillation bandwidths are the overall bandwidths determined along the line of drift, i.e. they approximate to the bandwidths expected in the absence of frequency drifting (Sutton 1971).

The pulsars selected for observation formed a reasonably consistent set in which the scintillation bandwidth generally lay between 100 kHz and 5 MHz, so that drifting patterns could clearly be seen in the available bandwidth. Of the 63 pulsars observed, 32 had a sufficient signal-to-noise ratio for any pattern drifting to be seen in the correlation function. Details of the frequency drift rates are given in Table 1. The measurement error on the scintillation parameters is of order 20 per cent. For high rates of drift (where the time interval between extreme frequency bands was too low for accurate measurement) such measurements give only a lower limit to the drift rate.

Table 1. Characteristics of pulsar scintillation spectra.

Pulsar	Dist (kpc)	$\Delta f_{1/2}$ (MHz)	τ (s)	V_s (km s^{-1})	Drift (kHz s^{-1})	log C_n^2 ($m^{-6.67}$)	m cos
0031−07	0.39	4	2300	26	+0.8	−3.97†	0.77
0149−16	0.44	>4	1100	>57	−4.4	−4.07†	
0301+19	0.56	0.6	900	30	+1.6	−2.97	0.15
0320+39	0.88	0.2	580	34	−0.4	−3.54†	0.30
0329+54★	2.30	0.03	330	37	+2.0	−3.94	0.016
0355+54★	1.60	(0.02)	110	94	(−0.3)	−2.56	(0.021)
0450−10	1.60	4	800	149	−17	−3.71	0.10
0525+21★	2.00	0.09	160	125	−1.8	−3.54	0.11
0628−28	1.30	0.5	460	82	−2.1	−4.09	0.18
0809+74	0.17	4	1000	39	−7	−3.98	0.20
0820+02	0.79	⩾4	1400	>60	>20	−3.38	
0823+26	0.71	0.5	200	140	+4.4	−3.64	0.20
0834+06	0.43	1.6	370	106	+7	−3.06	0.22
0919+06	1.00	0.5	270	123	+3	−3.02	0.22
0942−13	0.42	4	1600	38	+3	−4.03†	0.29
0950+18	0.09	⩾4	1500	>19	>50	−2.91	
1133+16	0.15	1.3	240	86	>20	−2.94	
1237+25	0.33	>4	750	>72	>70	−3.66	
1508+55	0.73	0.8	180	200	−4	−3.39	0.39
1604−00	0.36	>4	1000	>56	−4	−3.34	
1642−03	1.30	0.1	100	170	+3	−3.37	0.12
1702−18	0.74	(0.4)	220	116	(+7)	−3.65†	(0.09)
1706−16	0.81	0.4	640	42	(+3)	−3.72†	(0.07)
1749−28	1.00	>4	1300	>72	−17	−2.40	
1919+21	0.33	0.9	320	80	+6	−2.29	0.17
1929+10	0.08	2.2	490	40	−2.6	−1.97	0.61
1944+17	0.43	(0.3)	380	44	+0.5	−2.50	(0.56)
1952+29	0.20	>4	920	>46	−6	−2.91	
2016+28	1.30	0.3	760	39	+1.2	−3.48	0.12
2020+28	1.30	0.6	320	130	+3.2	−3.60	0.21
2021+51	0.68	0.4	430	57	+2.7	−3.58†	0.12
2045−16	0.38	1.6	160	229	−20	−3.47	0.18

Notes:
Distances from Manchester & Taylor (1981).
★ Pulsar observed at 960 MHz; $\Delta f_{1/2}$, τ, and drift rate scaled to 408 MHz via ν^4, ν^1, and ν^3 respectively (scaling weakly dependent on the value of α).
† Value of C_n^2 derived from the data (otherwise from Cordes *et al.* 1985).
Doubtful values are shown in parentheses.

For some pulsars our observations were taken at several epochs. In the case of PSR 1929+10, we find that the drift rate varies remarkably little and also persists in the same sense over the whole period of observation from 1981 December to 1982 June (see Fig. 2, where observations of two other pulsars are also shown). With these scattered observations we can at present assign only a rough time-scale of order six months to the variations. Since the velocities of scintillation patterns are of order 100 km s^{-1}, the lateral structure of the drift-rate pattern must then be of order 10^{12} m.

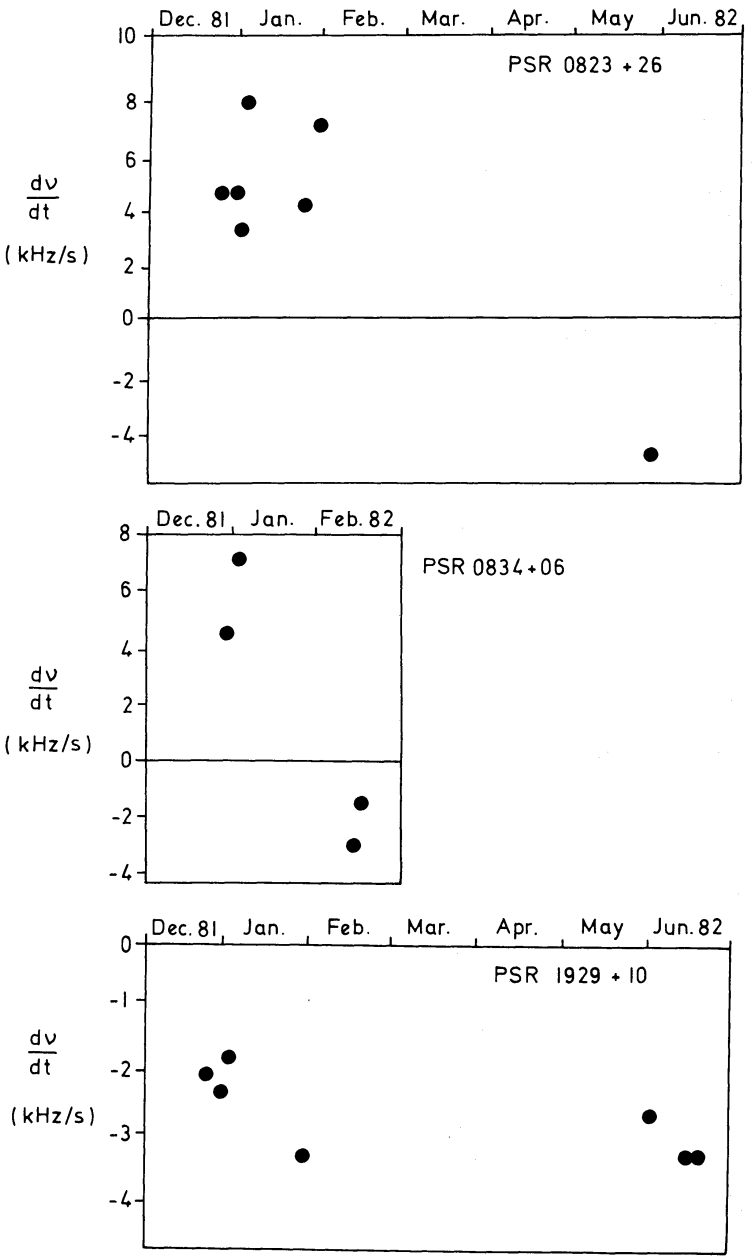

Figure 2. Temporal variations in the spectral feature drift rates of three pulsars.

3 Theory

3.1 THE ANGULAR SPREAD OF RAYS

The effect of irregularities in electron density in the interstellar medium may be regarded as an angular spreading of rays (or waves) from the radio source. Scheuer (1968) showed that the angular spread θ for a path length z containing irregularities with scale a and mean square deviation electron density $\langle \Delta n_e^2 \rangle$ varies as

$$\theta \propto (\langle \Delta n_e^2 \rangle)^{1/2} \times \lambda^2 \times \left(\frac{z}{a} \right)^{1/2}. \tag{1}$$

The contributions to θ from various scales of irregularity depend on the variation of $\langle \Delta n_e^2 \rangle$ with a, i.e. with the spectrum of the irregularities. Moreover, the effect of the spread of ray directions is

qualitatively different for large and small scales. A range of scales which in our observations at 408 MHz covered about two decades is responsible for typical scintillation, in which the observed flux varies over times of order 30 min and over a typical bandwidth of order 1 MHz. Larger scales of irregularity, however, effectively tilt the whole wavefront; it is the dispersion in this refraction that is responsible for frequency drifting (Sutton 1971; Hewish 1980). We designate θ_s as the angular spread of rays contributing to scintillation, and θ_r as the refraction angle due to large-scale iregularities and responsible for frequency drift.

The angle θ_s may under some circumstances be large enough for direct measurement: the apparent angular diameter of the Crab Pulsar has, for instance, been measured by interferometry at several frequencies (summarized by Mutel *et al.* 1974). Usually, however, it is obtained indirectly from the lateral scale of intensity variations and from the scintillation bandwidth, which is an effect of the extra path traversed by the deviated rays (Scheuer 1968; Rickett 1977).

In our observations we have measured intensity auto-covariance functions for both frequency and time, and found the time and frequency intervals $\tau_{1/2}$ and $\Delta f_{1/2}$ where the correlation falls to ½. It is more usual to measure τ_e, the time interval at which the correlation falls to $1/e$; we therefore calculated this from the relation $\tau_e = 1.2\,\tau_{1/2}$. The scale of the pattern on the ground is $V_s\tau_e$, where V_s is the pattern speed. This scale is related to the scattering angle θ_s by $\theta_s = \lambda(\sqrt{2}\times 2\pi \times V_s \times \tau_e)^{-1}$ as set out by Lee & Jokipii (1976). [Note that this equation without the factor $\sqrt{2}$, as used by Lee (1976), refers to correlation between fields rather than intensities.]

The extra path traversed by rays arriving at angle θ_s depends on the distance z of the source and on the distribution of irregularities along the ray path. For a simple thin diffracting screen half-way between the source and the observer, the extra path is $\frac{1}{2}z\theta_s^2$. The frequency interval $\Delta f_{1/2}$ is related to the delay δ by $\Delta f_{1/2} = (2\pi\delta)^{-1}$, so that for the simple halfway screen, and also for a uniformly filled path. $\Delta f_{1/2} = c(\pi z\theta_s^2)^{-1}$. [References to Lee & Jokipii (1976), Lee (1976) and Roberts & Ables (1982), show some inconsistencies in expressions for this relationship.] If the irregularities are concentrated near the Earth then $\Delta f_{1/2}$ is larger for a given θ_s, while $\Delta f_{1/2}$ is smaller if the irregularities are concentrated near the source. For example, Roberts & Ables (1982) used the relation $\Delta f_{1/2} = 2.5\,c(\pi z\theta_s^2)^{-1}$, corresponding to a concentration in the quarter of the path closest to the Earth.

This dependence on the distribution of irregularities, compounded with any remaining uncertainties about the theory, has fortunately been resolved by previous observations. Lyne & Smith (1982) measured the bandwidth and scintillation time-scale for 20 pulsars and derived a tranverse speed of the scintillation pattern for comparison with pulsar velocities directly measured by their proper motions. Using the measures $\Delta f_{1/2}$ and τ_e, they obtained a good correspondence between derived and measured velocities: they used the relations

$$\Delta f_{1/2} = c(\pi z\theta_s^2)^{-1} \tag{2}$$

$$\Delta\tau_e = \lambda(2\sqrt{2}\pi\theta_s)^{-1}. \tag{3}$$

We use the same formulae in this paper.

3.2 FREQUENCY DRIFTING

The pattern of phase and amplitude scintillatons due to the small-scale irregularities is displaced laterally by the large-scale pattern of angular deviations in the wavefront. The displacement is frequency-dependent due to dispersion in the refractive index along the path. Hewish (1980) analysed the effect in terms of refraction in a single large electron cloud: the effect is, however, more general. Consider a ray traversing a path uniformly filled with irregularities and arriving at angle θ_r to the line-of-sight. If the ray followed a uniformly curved path, its lateral displacement

would be $\frac{1}{2}z\theta_r$, and the frequency dispersion of this lateral displacement can then easily be found from the dispersion law

$$\frac{d\theta_r}{\theta_r} = -2\frac{d\nu}{\nu}. \tag{4}$$

The combined velocity of the source and the Earth gives a pattern speed V_s past the observer, so that $V_s = ds/dt$ where $ds = \frac{1}{2}z\,d\theta_r$. Thus the rate of frequency drifting is

$$\frac{d\nu}{dt} = \frac{\nu V_s \sec\phi}{\theta_r z}, \tag{5}$$

where ϕ is the angle between the plane of maximum frequency dispersion and the direction of pattern velocity.

In reality the arrival angle θ_r is the integral of small deviations along the line-of-sight: if the irregularities are distributed randomly throughout the line-of-sight, the differential relation of equation (5) still holds, although the total lateral deviation of the ray may be less than $\frac{1}{2}z\theta_r$.

Following Lee (1976) and Rickett (1977) we tentatively represent the spectrum $P(q)$ of electron density fluctuations by a modified power law in terms of wavenumber q, so that

$$P(q) = C_n^2 \frac{\exp(-q^2 l_p^2)}{(1+q^2L^2)^{\alpha/2}}, \tag{6}$$

where L and l_p are the outer and inner scales of the spectrum respectively and α is the spectral index. If l_p is assumed to be small, the exponential may be set to unity. This is often approximated to a simple power-law

$$P(q) = C_n^2 (qL)^{-\alpha}. \tag{7}$$

The index α is 11/3 for Kolmogorov turbulence.

Only restricted ranges of wavenumber q contribute effectively to the scintillation angle θ_s and the refraction angle θ_r. Fig. 3, after Roberts & Ables (1982), shows limits of scale a and scattering

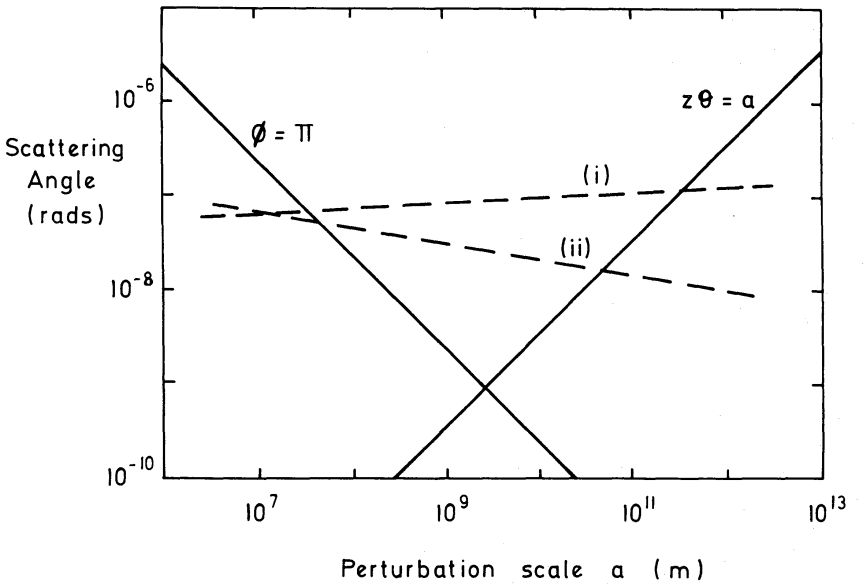

Figure 3. The variation of scattering angle with perturbation scale size. The areas above the solid lines ($\phi = \pi a$ and $z\theta = a$, where $z = 0.1$ kpc) represent the conditions necessary for strong scintillation and multipath respectively. The dashed line (i) represents an ISM with $\alpha > 4$, and (ii) an ISM with $\alpha < 4$.

angle θ for scintillation (note that the scattering angle is the angle of refraction for phase-front perturbations concentrated at size a). Beyond the left-hand limit the phase fluctuations are less than π and scintillation would not be deep, while the right-hand limit is the limit for multiple scattering. To the right of this limit the irregularities contribute only to θ_r. The geometric range of scale sizes a contributing to θ_s, i.e. between the two limit lines, is approximately equal to the inverse relative bandwidth $\nu/\Delta f_{1/2}$ of the scintillation pattern: this may be seen from Fig. 3, since $\Delta f_{1/2} \approx \nu$ at the intersection of the two limit lines, which have slopes of $+1$ and -1.

The analysis of our data is intended to show that the two phenomena of scintillation and frequency drifting are connected as in the theory outlined above. We already know that θ_s depends on distance z and wavelength λ more or less as expected from equation (1). The following discussion of our observations now shows that θ_r is similarly proportional to $\lambda^2 z^{1/2}$, in accordance with the postulated association of large- and small-scale irregularities. We then obtain ratios of θ_r and θ_s to compare with the ratio expected from the power-law spectrum.

4 Discussion

Our first test of the theory involves a direct comparison between rate of frequency drift and the velocity of the pulsar. We already know that for most pulsars the small-scale turbulence is fairly uniformly distributed along the propagation path, since the velocity of the scintillation pattern is approximately equal to the velocity of the pulsar (Lyne & Smith 1982). We now compare the rate of frequency drift with the scintillation velocities obtained from the following formula (valid at 408 MHz only)

$$V_s = 4.8 \times 10^4 (z \Delta f_{1/2})^{1/2} \tau^{-1} \text{ km s}^{-1} \quad (8)$$

where z, $\Delta f_{1/2}$, and τ have units of kpc, MHz, and s respectively (Lyne & Smith 1982). Fig. 4 is a plot of $d\nu/dt$ against V_s, omitting values which are limits only. Some scatter is expected because of

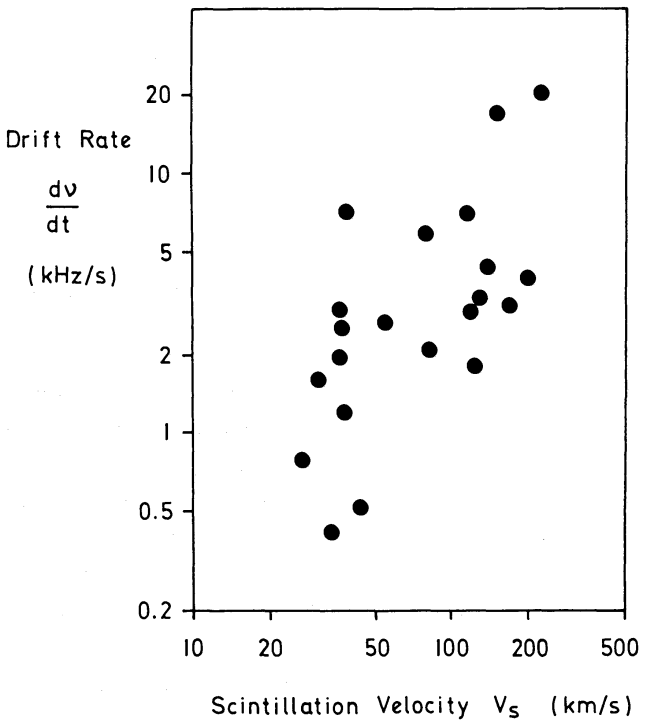

Figure 4. The variation of spectral feature drift rate with scintillation pattern velocity.

the factors z and $\sec\phi$ in equation (5), but there is nevertheless a good correlation indicating that the large-scale turbulence is also distributed along the propagation path.

We can also test the relationship between dv/dt and pulsar distance z. From equations (1) and (5) we expect to find $dv/dt \propto V_s z^{-3/2}$. Since derivations of the velocity V_s themselves use scintillation parameters, we prefer initially to plot dv/dt against z, as in Fig. 5, where we use values of z from Manchester & Taylor (1981). Bearing in mind the scatter expected from the factor V_s, there is a reasonable correlation, although the slope for our sample of pulsars is somewhat less steep than expected.

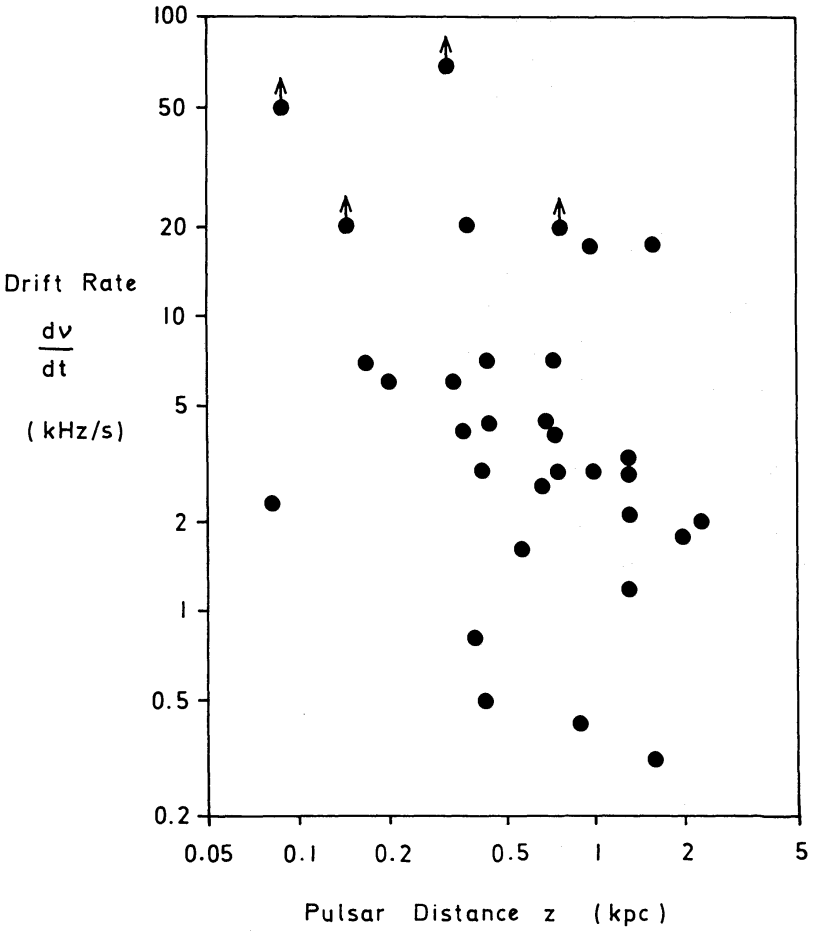

Figure 5. The variation of spectral feature drift rate with pulsar distance.

The variation with z is more precisely tested by plotting $V_s^{-1}\, dv/dt$ against z. Since we know that the levels of turbulence (C_n^2) along the lines-of-sight vary considerably between different pulsars at similar distances (Cordes, Weisberg & Boriakoff 1985) we also include this effect by plotting $(C_n^2)^{1/2} V_s^{-1}\, dv/dt$ as in Fig. 6. The factor $(C_n^2)^{1/2}$ is required because $dv/dt \propto \theta_r^{-1}$ for given values of z and V_s, and $\theta_r \propto (C_n^2)^{1/2}$. The slope of this graph is now close to -1.5, as expected. As noted above, some caution is needed in interpreting this more comprehensive plot, since the derivations of V_s and $(C_n^2)^{1/2}$ both involve the distance z, and some degree of correlation may be introduced artificially.

Having established that the large and small irregularities are closely associated, we can compare observed values of θ_s and θ_r so as to define the spectrum of turbulence more closely. If we put $\theta_r = m\,\theta_s$, m is a measure of the relative influence of large- and small-scale turbulence.

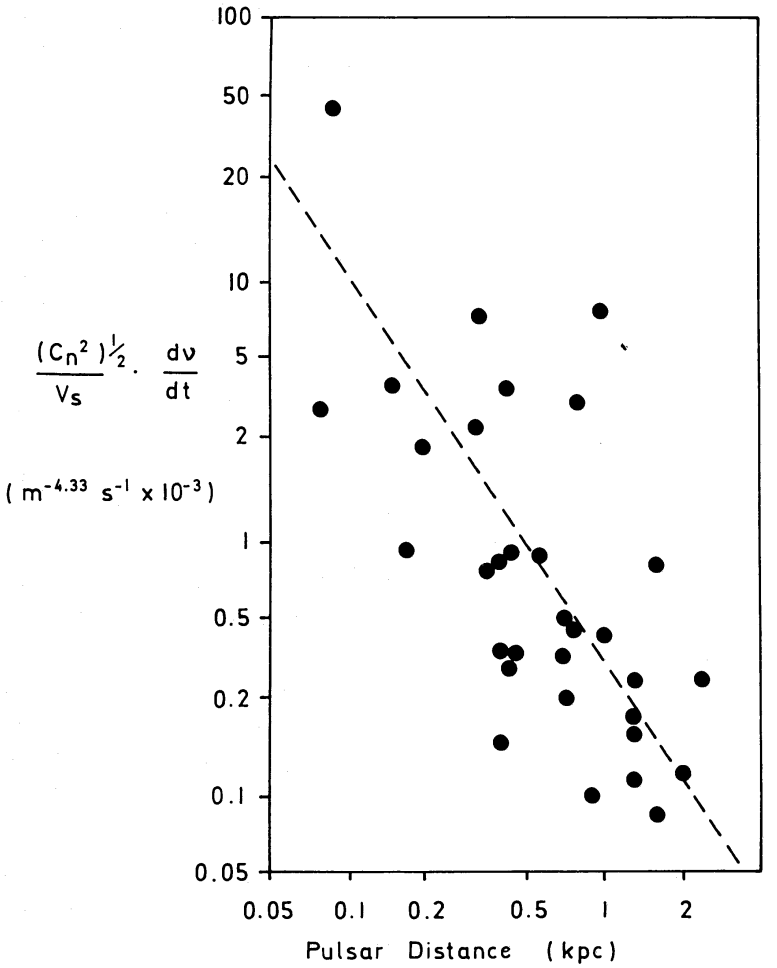

Figure 6. The variation of drift rate × turbulence/scintillation velocity with pulsar distance. The expected slope of −1.5 is indicated by the dashed line.

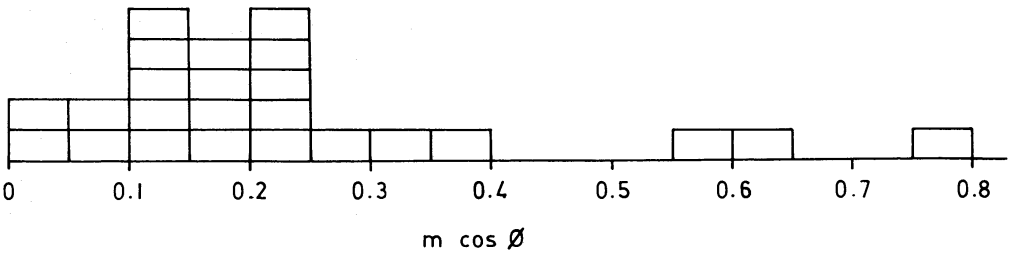

Figure 7. Histogram of values of $m\cos\phi$.

Taking account of the alignment angle ϕ, equations (2) and (5) give

$$m\cos\phi = \frac{\Delta f_{1/2}}{\sqrt{8}}\tau^{-1}\left(\frac{d\nu}{dt}\right)^{-1}. \tag{9}$$

We should emphasize that our values of $\Delta f_{1/2}$ refer to the bandwidth *along* the line of drift, and not the instantaneous bandwidth, which is reduced by dispersive refraction, as pointed out by Hewish (1980).

Derived values of $m\cos\phi$ are given in Table 1 and plotted as a histogram in Fig. 7. The spread in values suggests that it is reasonable to take the average value of m as

$$\bar{m} = \frac{\pi}{2}\overline{m\cos\phi} = 0.37. \tag{10}$$

In an Appendix we analyse an additional effect on the observed bandwidth which applies to larger values of m, and which suggests that the correct value is about 10 per cent larger than our value.

5 Limits on the spectrum of turbulence

Having established the connection between θ_r and θ_s we now refer back to the theoretical spectrum of turbulence in Section 4 above. Roberts & Ables (1982), using the simplified spectrum $P(q) \propto q^{-\alpha}$, showed that the scintillation angle θ_s is related to the limiting values of a by

$$\theta_s \propto [a_{\max}^{\alpha-4} - a_{\min}^{\alpha-4}]^{1/2}. \tag{11}$$

The limiting values correspond to the limit lines in Fig. 3. For θ_r the limits run from $a_{\max}$ to an unknown outer scale a^0.

The ratio $a_{\max}/a_{\min}$ is found approximately from $v/\Delta f_{1/2}$, where $\Delta f_{1/2}$ is of order 0.1 to 4 MHz at 408 MHz. As pointed out by Roberts & Ables (1982), the main contribution to the integral depends on the value of α. For $\alpha = 11/3$ as expected in the Kolmogorov spectrum, and indeed as for any value of α less than 4, the smaller scales are favoured, so that $\theta_s \propto a_{\min}^{(\alpha-4)/2}$, while $\theta_r \propto a_{\max}^{(\alpha-4)/2}$. We therefore expect, for a Kolomogorov spectrum, values of m between $4000^{-1/6} \simeq 0.25$ and $200^{-1/6} \simeq 0.46$.

This range for m is gratifyingly close to our observational result, although it will be obvious that the coincidence is not an unequivocal test of the theory, since we have assumed that the outer scale parameter a_0 does not affect the result. It is possible to obtain the same theoretical ratio by using a lower value of α, i.e. a flatter spectrum, and applying a cut-off at a suitable outer scale.

The persistence of the drifting patterns for several months (Section 2) shows that the large scale involved is at least 10^{12} m, considerably larger than $a_{\max}$ which is of order 10^{10} m. Our result therefore suggests strongly that the spectrum of irregularities persists as a continuous spectrum to scales greater than 10^{12} m, and that the spectral index α is close to 11/3, in agreement with the Kolmogorov value favoured by other characteristics of scattering. We note, however, that the quasi-periodic scintillation patterns observed in some pulsars suggest that the larger scales of irregularity may occasionally be greater than expected from the Kolmogorov spectrum. We are grateful to Professor A. Hewish for discussions on this point.

References

Armstrong, J. W. & Rickett, B. J., 1981. *Mon. Not. R. astr. Soc.*, **194,** 623.
Cordes, J. M., Weisberg, J. M. & Boriakoff, V., 1985. *Astrophys. J.*, **288,** 221.
Ewing, M. S., Batchelor, R. A., Friefeld, R. D., Price, R. M. & Staelin, D. H., 1970. *Astrophys. J.*, **162,** L169.
Hewish, A., 1980. *Mon. Not. R. astr. Soc.*, **192,** 799.
Lee, L. C., 1976. *Astrophys. J.*, **206,** 744.
Lee, L. C. & Jokipii, J. R., 1975. *Astrophys. J.*, **196,** 695.
Lee, L. C. & Jokipii, J. R., 1976. *Astrophys. J.*, **206,** 735.
Lyne, A. G. & Smith, F. G., 1982. *Nature,* **298,** 825.
Manchester, R. N. & Taylor, J. H., 1977. *Pulsars*, Freeman, San Francisco.
Manchester, R. N. & Taylor, J. H., 1981. *Astr. J.*, **86,** 1953.
Mutel, R. L., Broderick, J. J., Carr, T. D., Lynch, M., Desch, M., Warnock, W. W. & Klemperer, W. K., 1974. *Astrophys. J.*, **193,** 279.
Rickett, B. J., 1977. *Ann. Rev. Astr. Astrophys.*, **15,** 479.
Rickett, B. J., Coles, W. A. & Bourgois, G., 1984. *Astr. Astrophys.*, **134,** 390.
Roberts, J. A. & Ables, J. G., 1982. *Mon. Not. R. astr. Soc.*, **201,** 1119.
Scheuer, P. A. G., 1968. *Nature,* **218,** 920.
Shishov, V. I., 1973. *Astr. Zh.*, **50,** 941 (*Soviet Astr.*, **17,** 598).
Sutton, J., 1971. *Mon. Not. R. astr. Soc.*, **155,** 51.

Appendix: The effect of large values of $m=\theta_r/\theta_s$

Large values of dispersive refraction may reduce the observed scintillation bandwidth Δf_{obs} below the value $\Delta f_{1/2}$ appropriate to scattering through the angle θ_s, as given by (3) above. This occurs when the region of coherence on the ground, i.e. a typical patch of high intensity, is drawn out by dispersion within the bandwidth $\Delta f_{1/2}$ to an extent large compared with its own width.

The pattern scale on the ground is $(\sqrt{8}\pi)^{-1}\lambda\theta_s^{-1}$, and the scale of refractive dispersion over the bandwidth $\Delta f_{1/2}$ is

$$\frac{z}{2}\Delta f_{1/2}\frac{d\theta_r}{dv}=z\Delta f_{1/2}\frac{\theta_r}{v}.$$

If this latter scale is large compared with the pattern scale, then the observed bandwidth will depend on the direction of the velocity. Since $\Delta f_{1/2}=c(\pi z\theta_s^2)^{-1}$, this condition is

$$m=\frac{\theta_r}{\theta_s}>8^{-1/2}=0.35.$$

Clearly some account must be taken of this effect even if $m=0.35$, but it is a small effect at this level.

We now consider what happens if m is much larger, so that within $\Delta f_{1/2}$ the blobs are stretched out much further than their width. The limiting angle $\phi_0=\cot^{-1}(8^{1/2}m)$ between pattern velocity and the direction of dispersion is now small, and we can for the moment ignore any pulsars whose velocity vectors lie below ϕ_0, i.e. all those for which our analysis properly applies. Then a velocity vector at ϕ will give a reduced observed bandwidth B_{obs} such that

$$\frac{\cot\phi}{\cot\phi_0}\approx\frac{\Delta f_{obs}}{\Delta f_{1/2}}.$$

Then our equation (9) becomes

$$m\cos\phi=\Delta f_{obs}\cot\phi_0\tan\phi\,8^{-1/2}\tau^{-1}\left(\frac{dv}{dt}\right)^{-1}$$

and our observed data give $m\times\cos\phi\times\cot\phi\times\tan\phi_0$ instead of the required $m\cos\phi$. Since $\tan\phi_0$ corresponds to the relative scales arising from diffraction and refraction, we find $\tan\phi_0=(m\sqrt{8})^{-1}$.

The mean apparent value of $m\cos\phi$ is then found by integrating this expression from ϕ_0 to $\pi/2$ and integrating $m\cos\phi$ from 0° to ϕ_0, giving

$$\frac{1}{\sqrt{8}}\times\frac{2}{\pi}\left[-\log_e\left(\tan\frac{\phi_0}{2}\right)-\cos\phi_0+\sqrt{8}m\sin\phi_0\right]=-0.225\log_e\tan\frac{\phi_0}{2}.$$

Following the procedure of this paper we would therefore find apparent values of m as follows:

m_{actual}	0.2	0.35	0.5	1.0
$m_{apparent}$	0.19	0.31	0.41	0.62

We conclude that our result $m=0.37$ needs little correction for this effect.